Paramagnetic Ce^{3+} optical emitters in garnets: Optically detected magnetic resonance study and evidence of Gd-Ce cross-relaxation effects

D. O. Tolmachev,[1] A. S. Gurin,[1] Yu. A. Uspenskaya,[1] G. R. Asatryan,[1] A. G. Badalyan,[1] N. G. Romanov,[1,*] A. G. Petrosyan,[2] P. G. Baranov,[1,3] H. Wieczorek,[4] and C. Ronda[4]

[1]*Ioffe Institute, St. Petersburg, 194021, Russia*

[2]*Institute for Physical Research, National Academy of Sciences of Armenia, Ashtarak-2, 0203, Armenia*

[3]*Peter the Great St. Petersburg Polytechnic University, St. Petersburg, 195251, Russia*

[4]*Philips Research, High Tech Campus 4, 5656 AE, Eindhoven, The Netherlands*

(Received 25 March 2015; revised manuscript received 21 March 2017; published 12 June 2017)

Paramagnetic Ce^{3+}optical emitters have been studied by means of optically detected magnetic resonance (ODMR) via Ce^{3+} spin-dependent emission in cerium-doped garnet crystals which were both gadolinium free and contain gadolinium in a concentration from the lowest (0.1%) to 100%, i.e., to the superparamagnetic state. It has been shown that the intensity of photoluminescence excited by circularly polarized light into Ce^{3+} absorption bands can be used for selective monitoring the population of the Ce^{3+} ground-state spin sublevels. Direct evidence of the cross-relaxation effects in garnet crystals containing two electron spin systems, i.e., the simplest one of Ce^{3+} ions with the effective spin $S = \frac{1}{2}$ and the system of Gd^{3+} ions with the maximum spin $S = \frac{7}{2}$, has been demonstrated. Magnetic resonance of Gd^{3+} has been found by monitoring Ce^{3+} emission in cerium-doped garnet crystals with gadolinium concentrations of 0.1 at. %, 4%–8%, and 100%, which implies the impact of the Gd^{3+} spin polarization on the optical properties of Ce^{3+}. Strong internal magnetic fields in superparamagnetic crystals were shown to modify the processes of recombination between UV-radiation-induced electron and hole centers that lead to the recombination-induced Ce^{3+} emission. Observation of spikes and subsequent decay in the cross-relaxation-induced ODMR signals under pulsed microwave excitation is suggested to be an informative method to investigate transient processes in the many-spin system of Ce^{3+}, Gd^{3+}, and electron and hole radiation-induced centers.

DOI: 10.1103/PhysRevB.95.224414

I. INTRODUCTION

The $5d$-$4f$ transitions of Ce^{3+} in garnets produce an emission of quantum efficiency close to unity in a broad band, extending from 500 to about 650 nm. The system is ideally suited for luminescence conversion of blue light emitting diodes (LED) [1,2]. The phosphor absorbs part of the blue light emitted by a LED and converts the blue light into yellow emission, which, together with transmitted blue light, yields white light.

Cerium-doped garnet crystals have a high potential as high-performance scintillators for numerous applications including nuclear physics and modern medical imaging methods [3–6]. Ce-doped gadolinium containing garnets have extremely high photon gain, a high density, and, as a result, a high stopping power, which is a considerable advantage for their scintillator applications. The underlying idea is that Gd^{3+} ions are involved in the energy transfer to Ce^{3+} ions.

It was shown that rare-earth-doped crystals are excellent hardware for quantum information processing in the solid state. High-fidelity optical initialization, efficient coherent manipulation, and optical readout of a single-electron spin of Ce^{3+} ion in a yttrium aluminum garnet (YAG) crystal have been demonstrated and a possibility of all-optical addressing and coherent control of single Ce^{3+} spin-based quantum bits has been proven [7–9]. Additional functionality of these materials is added by their waveguiding properties allowing for on-chip photonic networks. Strong hyperfine coupling to aluminum nuclear spins suggests that cerium electron spins can be exploited as an interface between photons and long-lived nuclear spin memory. Recent electron spin echo detected electron-nuclear double resonance study of cerium-doped garnet ceramics allowed estimating the hyperfine interactions with the surrounding Al nuclei [10].

Obviously, progress in applications of cerium-doped garnets depends in many respects on the degree of understanding of the spectroscopic properties of these crystals and, on this basis, the development of methods for producing crystals with desired parameters. One of the most powerful and direct methods to investigate the properties of materials is electron paramagnetic resonance (EPR) [11,12], which makes it possible to determine the chemical and charge states of an impurity center, its local symmetry, the composition of the nearest environment, the structure of energy levels, the specific features of the interaction with the crystal lattice, etc.

EPR spectra of Ce^{3+} ions located in the regular environment in YAG:Ce crystals [13] and the family of Ce^{3+} ions in the immediate vicinity of which there are permutation defects [14] were investigated. Defect states in cerium-doped lutetium garnet (LuAG) crystals $Lu_3Al_5O_{12}$ were studied [15] and the effect of light irradiation on the Ce^{3+} EPR spectra was found. EPR studies of Gd^{3+} in garnets have been performed [16,17], but the reported spin Hamiltonian parameters for Gd^{3+} in YAG differed significantly both in value and even in sign. The revised spin Hamiltonian parameters for Gd^{3+} in YAG have been recently reported [18] as well as the parameters for Gd^{3+} in LuAG crystals [19]. EPR of gadolinium garnet crystals has been studied in a large range of temperatures and frequencies and the shape of the broadened EPR line was analyzed [20].

*nikolai.romanov@mail.ioffe.ru

For single-spin manipulation, one needs to use optically detected magnetic resonance (ODMR) techniques that provide extremely high sensitivity, spatial and spectral resolution. ODMR [21–25] is based on the dependence of optical properties on the electron spin polarization of paramagnetic centers, which are involved in the optical pumping cycle or a competing spin-dependent nonradiative process.

ODMR of cerium ions Ce^{3+} in garnets was studied via the magnetic circular dichroism (MCD) of the absorption [26,27]. Using ODMR, the absorption bands of Ce^{3+} at 227, 270, 338 nm and at 458.5 nm in YAG:Ce have been definitely identified [27]. ODMR of a single Ce^{3+} was recently observed via photoluminescence (PL) using strong optical pumping into the Ce^{3+} zero-phonon line [8,9].

The electron spin polarization can be influenced directly by microwave-induced resonant transitions between the spin sublevels at EPR, but also due to cross relaxation [28] of a center with another paramagnetic center. Optically detected cross relaxation has been observed in many different systems both via MCD [29–31] and via photoluminescence [32,33]. Since both Ce^{3+} and Gd^{3+} are paramagnetic, the spin-dependent optical properties of garnets containing Ce^{3+} and Gd^{3+} can be influenced by their interaction and cross relaxation.

In preliminarily irradiated gadolinium garnet crystals $Gd_3Ga_3Al_2O_{12}$:Ce (0.1% Ce), a giant magnetic field effect on spin-dependent recombination afterglow has been recently found and ascribed to huge internal magnetic fields created by the magnetic moments of the unpaired electrons of the gadolinium ions and cross relaxation between the spin sublevels of the gadolinium ions Gd^{3+} and the levels of radiation-induced electron or hole centers [34].

In this paper, we report results of a study of Gd^{3+} emitters in cerium-doped garnet crystals and in garnet crystals containing Ce^{3+} and Gd^{3+} by means of ODMR via photoluminescence. Preliminary results of this investigation have been partly reported in the conference papers [35,36]. In LuAG:Gd crystals studied [36], 4% to 8% of Lu^{3+} ions were replaced by Gd^{3+} ions and the broadening of EPR and ODMR lines and the absence of reliable spin Hamiltonian parameters of Gd^{3+} made the precise analysis of the Gd-Ce cross-relaxation processes difficult. In this study, three types of gadolinium-containing garnets have been investigated, i.e., YAG crystals with low Gd content (0.1 at. %), LuAG crystals with a medium Gd content (4 at. % and 8 at. %) and gadolinium garnets with 100% Gd. Observation of Ce^{3+} ODMR via the PL intensity under nonresonant circularly polarized excitation allowed monitoring selectively the population of one of two Ce^{3+} ground-state spin sublevels and revealing the Gd-Ce cross-relaxation effects in a large range of Gd concentrations in garnet crystals, from crystals with 0.1% Gd, where EPR lines are very narrow, to gadolinium garnets, in which high Gd concentration and strong internal magnetic fields result in a different behavior of spin-dependent processes.

II. SAMPLES AND EXPERIMENTAL DETAILS

We investigated cerium-doped $Y_3Al_5O_{12}$, $Y_3Al_5O_{12}$:Ce,Gd (0.1% Gd), $Lu_{2.875}Gd_{0.125}Al_5O_{12}$:Ce, $Lu_{2.75}Gd_{0.25}Al_5O_{12}$:Ce, and $Gd_3Ga_3Al_2O_{12}$ single crystals. They have been grown from the melt by vertical directed crystallization [37,38] in an Ar/H_2 atmosphere with the use of molybdenum containers and seed crystals oriented along the crystallographic axis [001]. The content of Ce in all crystals was ca. 0.1 at. % relative to Y. We mean the percentage widely used in laser physics, namely, number of atoms of dopant/number of atoms, which can be substituted with the dopant, e.g., for YAG:Ce crystals, this will be the fraction of yttrium (Y^{3+}) ions which have been replaced with Ce^{3+} ions. The samples were cut from the regions without facet growth forms and light-scattering inclusions in the form of a rectangular parallelepiped about $1 \times 2 \times 4\,mm^3$ in size.

Photoluminescence (PL) was excited by UV light of a deuterium arc lamp with appropriate filters in the range of 250 to 400 nm or a semiconductor laser. The PL spectra were measured at a temperature of 1.8 and 300 K with a photomultiplier in combination with a grating monochromator and corrected for the spectral response of the detection system. EPR experiments were carried out by using a commercial X-band (9.3-GHz) EPR spectrometer equipped with a helium gas-flow cryostat providing the temperature control within the range of 4–300 K.

ODMR spectra were recorded at a temperature of 1.5–2 K by monitoring the intensity of luminescence excited with circularly polarized light of a 405-nm laser followed by a quarter wave plate or by UV light of a deuterium arc lamp. The excitation light beam was directed along the magnetic field. The sample was placed in the cylindrical microwave cavity H_{011} with optical access for excitation and emission light. The maximum power of the Q-band (35 GHz) microwave generator was about 600 mW. In some ODMR experiments, a quasioptical microwave circuit [39] was used, which allowed the ODMR measurements at higher frequency in V-band (72 GHz) and W-band (94 GHz). No modulation of microwaves was used because of long spin-lattice relaxation times of the investigated paramagnetic centers.

III. RESULTS AND DISCUSSION

A. ODMR of Ce^{3+} in YAG:Ce via Ce^{3+} photoluminescence intensity

Figure 1(a) shows the PL spectrum of a $Y_3Al_5O_{12}$:Ce (0.1 at. % Ce) single crystal recorded at a temperature of 1.8 K under 405-nm excitation. The spectrum presents the Ce^{3+} emission bands broadened by electron-phonon interaction.

Ce^{3+} ($4f^1$) has only one $4f$ electron and presents the simplest example of the $5d$-$4f$ emission. The energy-level scheme for the Ce^{3+} free ion and Ce^{3+} in a garnet is shown in the inset in Fig. 1(a). The $4f^1$ ground-state and $5d^1$ excited-state levels are split as a result of the spin-orbit (SO) coupling and the crystal field. The ground-state $4f^1$ configuration yields two levels $^2F_{5/2}$ and $^2F_{7/2}$ which are separated by approximately 2000 cm^{-1}. At low temperatures and low Ce^{3+} concentrations, it is possible to observe the $5d \rightarrow 4f$ emission bands separated into two distinct peaks [8,40]. The real energy levels and the relative admixtures of the wave functions depend on parameters of the crystal field. For Ce^{3+} ions in YAG, the energy of the second and the third Kramers doublets of the $^2F_{5/2}$ manifold are elevated above the ground state by 228 and 587 cm^{-1}, respectively, and, as a result, EPR transitions are observable only between the

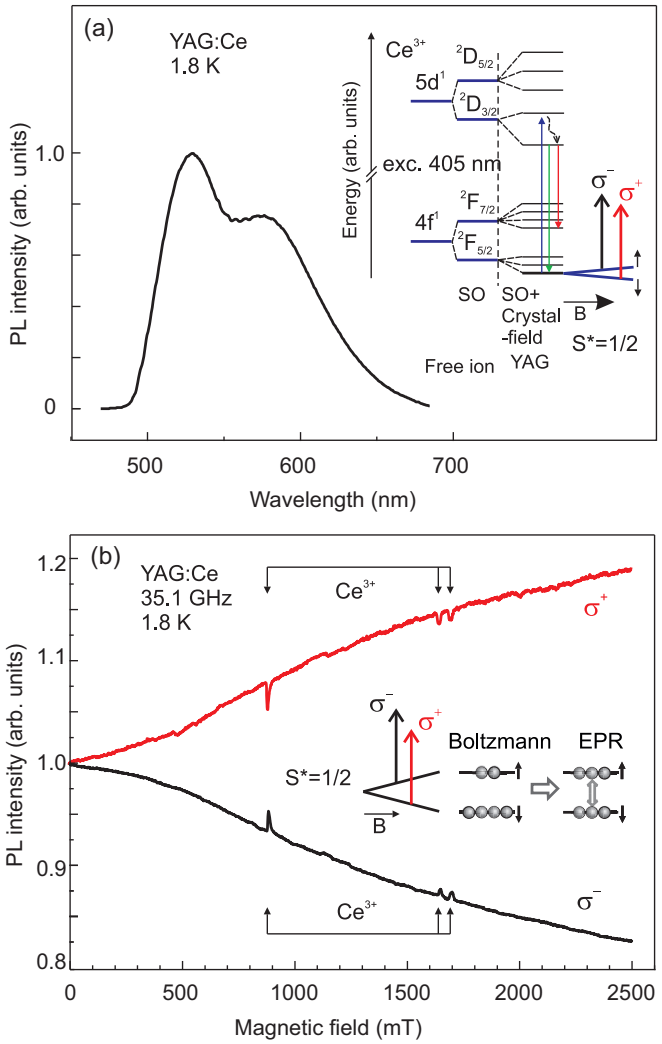

FIG. 1. The photoluminescence spectrum in $Y_3Al_5O_{12}$:Ce(0.1% Ce) single crystal recorded at a temperature of 1.8 K under 405-nm excitation. The energy levels of free ions and their splitting under the action of spin-orbit (SO) interaction and crystal field for Ce^{3+} in YAG are shown in inset. (b) Magnetic field dependencies of the Ce^{3+} PL intensity measured in $Y_3Al_5O_{12}$:Ce (0.1% Ce) single crystal at 1.8 K in the presence of the 35.1-GHz microwaves. The excitation light was circularly polarized as marked in the figure. The magnetic field orientation is close to [100]. Inset shows the Ce^{3+} ground-state levels in magnetic field and absorption of circularly polarized light.

components of the lowest doublet, which is only populated at low temperatures (below 20 K where EPR of Ce^{3+} can be detected).

Cerium has only even isotopes with a zero nuclear magnetic moment ($I = 0$). The EPR spectra and their angular dependencies can be described by the effective spin $S = \frac{1}{2}$ and an anisotropic g factor using the spin Hamiltonian of orthorhombic symmetry in the form

$$\hat{H} = \mu_B \vec{\boldsymbol{S}} \cdot \hat{g} \cdot \vec{\boldsymbol{B}}, \qquad (1)$$

where μ_B is the Bohr magneton, $\boldsymbol{S}$ is the effective spin ($S = \frac{1}{2}$), $\boldsymbol{B}$ is the external magnetic field, and $\hat{g}$ is the g tensor.

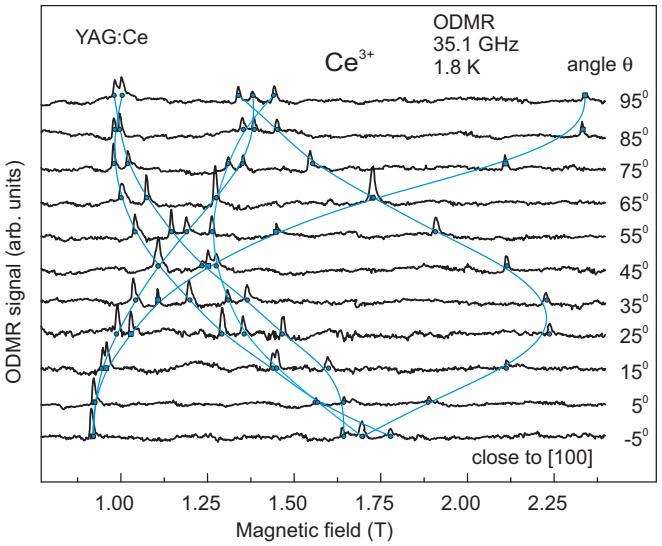

FIG. 2. Angular dependencies of the 35-GHz ODMR in $Y_3Al_5O_{12}$:Ce(0.1% Ce) recorded with rotation of the sample corresponding to $\varphi = 24^\circ$ and $\theta = -5^\circ$–95°, 10° increments. The ODMR spectra are baseline corrected. Solid lines are the results of calculations using (1).

In YAG single crystals, rare-earth ions occupy as a rule dodecahedral sites of the crystal lattice (c sites), thus replacing the Y^{3+} ions. In this position, the Y^{3+} ions are coordinated by eight oxygen ions with local symmetry D_2 and form six magnetically nonequivalent Ce^{3+} centers. In this study, the principal directions of the local magnetic axes have been chosen in such a way that the x axes are along one of the crystallographic directions $\langle 001 \rangle$ and the directions of the axes y and z coincide with the $\langle 110 \rangle$ directions. The corresponding Euler angles for one of the six centers in the dodecahedral position are as follows: $\alpha = 45^\circ$, $\beta = 90^\circ$, and $\gamma = 180^\circ$. The orientations of the other five Ce^{3+} centers can be obtained by the symmetry operations in the YAG crystal lattice.

In a magnetic field at a temperature of 1.8 K, the intensity of the total PL of $Y_3Al_5O_{12}$:Ce crystals was found to increase or decrease depending on the sign of circular polarization of the excitation light, i.e., σ^+ or σ^-, respectively, as shown in Fig. 1(b). Without the microwaves, these dependencies were in agreement with the Boltzmann populations of the Ce^{3+} ground-state levels. Application of 35-GHz microwaves resulted in appearance of anisotropic resonance signals, which corresponded to EPR in the ground state of Ce^{3+}. This was proven by measuring their angular variations shown in Fig. 2, where the 35-GHz ODMR spectra recorded in the YAG:Ce single crystal with rotation of the sample corresponding to $\varphi = 24^\circ$ and $\theta = -5^\circ$–95°, 10° increments, are displayed. In these spectra the baseline is subtracted. The parameters of the g tensor that have been obtained from the experimental orientation dependencies of the ODMR line positions: $g_x = 2.74 \pm 0.05$, $g_y = 1.87 \pm 0.05$, and $g_z = 0.91 \pm 0.05$ coincide with the data reported in [13,14] where EPR of Ce^{3+} was studied. Full lines in Fig. 2(a) are the result of calculations, which were performed with a special computer program developed by Grachev [41].

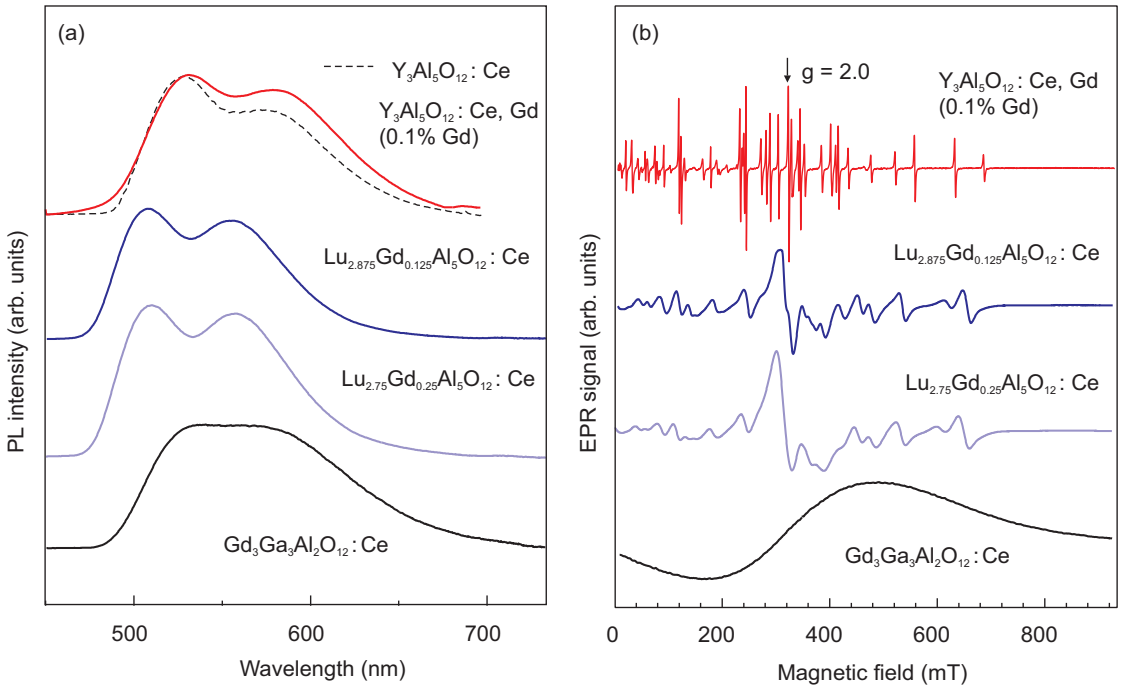

FIG. 3. (a) Photoluminescence (a) and EPR (b) spectra of the samples under study: $Y_3Al_5O_{12}$:Ce,Gd (0.1% Gd), $Lu_{2.875}Gd_{0.125}Al_5O_{12}$:Ce, $Lu_{2.75}Gd_{0.25}Al_5O_{12}$:Ce, and $Gd_3Ga_3Al_2O_{12}$:Ce. The Ce concentration was about 0.1% in all samples. Dashed line in (a) shows the PL spectrum in $Y_3Al_5O_{12}$:Ce for comparison. PL was excited with a 405-nm laser and the spectra were recorded at 1.8 K. The 9.3-GHz EPR spectra in (b) were recorded at RT with the crystal orientation close to [110].

It is known that Ce^{3+} ions in garnet crystals exhibit strong magnetic circular dichroism (MCD) in absorption [27]. MCD monitors the spin polarization of the Ce^{3+} ground state due to the spin selection rules, which lead to different absorption of right- and left-polarized light $\sigma^+$and σ^-. The spin polarization is normally determined by the Boltzmann population distribution and increases in magnetic field. EPR transitions tend to equalize populations of the levels in resonance and can therefore be detected as a decrease of the MCD absolute value.

Recently, ODMR of a single Ce^{3+} ion in YAG crystals was recorded via the intensity of photoluminescence [8,9]. To force the creation of a nonequilibrium population of spin sublevels in the ground state of cerium ions resonant circularly polarized optical excitation into the zero-phonon line of $Ce^{3+}$was used, which resulted in efficient pumping of the ion into $4f^1$ spin-up state and a reduction of the intensity of the phonon-assisted Ce^{3+}emission excited from the spin-down state.

In our experiments, circularly polarized excitation of Ce^{3+} luminescence was performed into the phonon broadened absorption band and no optical pumping effects were observed. This allowed monitoring separately the populations of the Ce^{3+} ground state $M_S = +\frac{1}{2}$ or $-\frac{1}{2}$ spin sublevels due to selective excitation from one or another level. Figure 1(b) (inset) shows the energy levels of the Ce^{3+} ground state in magnetic field and absorption of circularly polarized light. In magnetic field at low temperature, the lowest $M_S = -\frac{1}{2}$ (spin-down) level is preferentially populated due to Boltzmann population distribution. As a result, the intensity of luminescence increases in magnetic field when it is excited by σ^+ polarized light and decreases under σ^- excitation. Saturation of EPR transitions results in a decrease of population of the lowest $M_S = -\frac{1}{2}$ (spin-down) level and an increase of population of the $M_S = +\frac{1}{2}$ (spin-up) level and can be detected via the intensity of Ce^{3+} luminescence excited by σ^+ or σ^- polarized light, respectively, as shown in Fig. 1(b). Thus, the version of the ODMR techniques used in this study can be called MCD in photoluminescence excitation. It can be used for a study of cross-relaxation effects in crystals that contain other paramagnetic centers in addition to Ce^{3+}.

B. ODMR in cerium-doped garnet crystals containing two spin systems, i.e., Ce^{3+} ($S = \frac{1}{2}$) and Gd^{3+} ($S = \frac{7}{2}$)

1. Photoluminescence and EPR characterization of the samples

Three types of garnet crystals codoped with cerium and gadolinium have been studied in this work, i.e., $Y_3Al_5O_{12}$:Ce,Gd crystals with low Gd content (below 0.1 at. %), $(Lu,Gd)_3Al_5O_{12}$:Ce with medium Gd content (4 at. % and 8 at. %) and gadolinium garnet $Gd_3Ga_3Al_2O_{12}$:Ce with 100% Gd. PL and EPR spectra of the samples under study are shown in Figs. 3(a) and 3(b), respectively. PL spectra were measured at 1.8 K under 405-nm excitation. Only Ce^{3+} emission was observed in all samples. EPR spectra presented in Fig. 3(b) were measured at room temperature. They belong to Gd^{3+}.

The gadolinium trivalent ion Gd^{3+} has a half-filled electronic shell with a $4f^7$ configuration. The ground $^8S_{7/2}$ multiplet is characterized by an absence of orbital momentum ($L = 0$) and the spin momentum value of $S = \frac{7}{2}$. The eightfold-degenerate level of a free trivalent gadolinium ion being placed in the axial crystal field is split into four Kramers

doublets. For small concentrations of Gd^{3+} ions in garnets their EPR spectra can be described by a spin Hamiltonian

$$\hat{H} = g\mu_B(\boldsymbol{BS}) + 1/3\left(b_2^0 O_2^0 + b_2^2 O_2^2\right) + 1/60\left(b_4^0 O_4^0 + b_4^2 O_4^2 + b_4^4 O_4^4\right), \quad (2)$$

where O_n^m are Stevens operators [42] and m can be 0, 2, and 4.

Similar to Ce^{3+}, Gd^{3+} ions substitute for the Y^{3+} ions in YAG and Lu^{3+} in LuAG and occupy dodecahedral sites (c sites). There are six magnetically nonequivalent Gd^{3+} positions in the garnet crystal, therefore, for an arbitrary crystal orientation a superposition of six spectra is to be observed. For low concentrations of isolated Gd^{3+} ions in nonmagnetic crystals (e.g., garnet host crystals), the EPR spectrum consists of seven fine-structure lines for each of six magnetically nonequivalent centers. They result from both intradoublet and interdoublet transitions ($M_S = -\frac{7}{2} \leftrightarrow -\frac{5}{2}; -\frac{5}{2} \leftrightarrow -\frac{3}{2}; -\frac{3}{2} \leftrightarrow -\frac{1}{2}; -\frac{1}{2} \leftrightarrow +\frac{1}{2}; +\frac{1}{2} \leftrightarrow +\frac{3}{2}; +\frac{3}{2} \leftrightarrow +\frac{5}{2}; +\frac{5}{2} \leftrightarrow +\frac{7}{2}$) in the approximation of the strong magnetic fields.

In our calculations, we used the following parameters of the spin Hamiltonian (2) for Gd^{3+} YAG [18]: $g = 1.991, b_2^0 = 2275.3$ MHz, $b_2^2 = 717.9$ MHz, $b_4^0 = -130$ MHz, $b_4^2 = 16.9$ MHz, $b_4^4 = 591.4$ MHz. They describe well the EPR spectrum of Gd^{3+} in YAG containing 0.1% of Gd, which is shown in the upper part of Fig. 3(b) for the crystal orientation close to [110]. For Gd^{3+} in LuAG theses parameters are [19] $g = 1.991$, $b_2^0 = 1750$ MHz, $b_2^2 = 865$ MHz, $b_4^0 = -137$ MHz, $b_4^2 = 14$ MHz, $b_4^4 = 645$ MHz.

No Ce^{3+} EPR can be observed at room temperature, and only EPR spectra of Gd^{3+} are visible in Fig. 3(b). It is to be noted that due to the high concentration of gadolinium in the two LuAG samples (4% and 8%) the EPR spectra are characterized by broadened EPR lines. This broadening increases with the increase in the Gd content.

In Gd garnets $Gd_3Ga_3Al_2O_{12}$ (Gd 100%) a very wide EPR line is observed and the crystal-field splitting (fine structure) manifests itself in the wide wings of the line. The shape of the EPR line in gadolinium garnets at room temperature is explained using the Kubo-Toyabe model with the linewidth expected from the dipolar interactions [42]. It was shown [20] that at low temperature the line broadens with the increased magnetization and the linewidth is due to a wide distribution of local static fields.

2. *ODMR in cerium-doped YAG with small concentration of gadolinium (0.1%)*

Figure 4(a) presents the magnetic field dependencies of the Ce^{3+} PL intensity measured at a temperature of 1.8 K in YAG:Ce,Gd (0.1 at. % Gd). PL was excited by 405-nm circularly polarized light. Thick and thin lines correspond to different levels of the microwave power: 50 and 0.05 mW, respectively. Without the microwaves these dependencies are in agreement with the Boltzmann populations of the Ce^{3+} ground-state levels. Under the action of the microwave field ODMR signals of Ce^{3+} appear together with additional anisotropic ODMR lines, which can be ascribed to Gd^{3+}. The ODMR amplitudes increase with the increasing microwave power as shown in Fig. 4(a), and their dependencies on the detection wavelength coincide with the PL spectra, i.e., the Ce^{3+} emission.

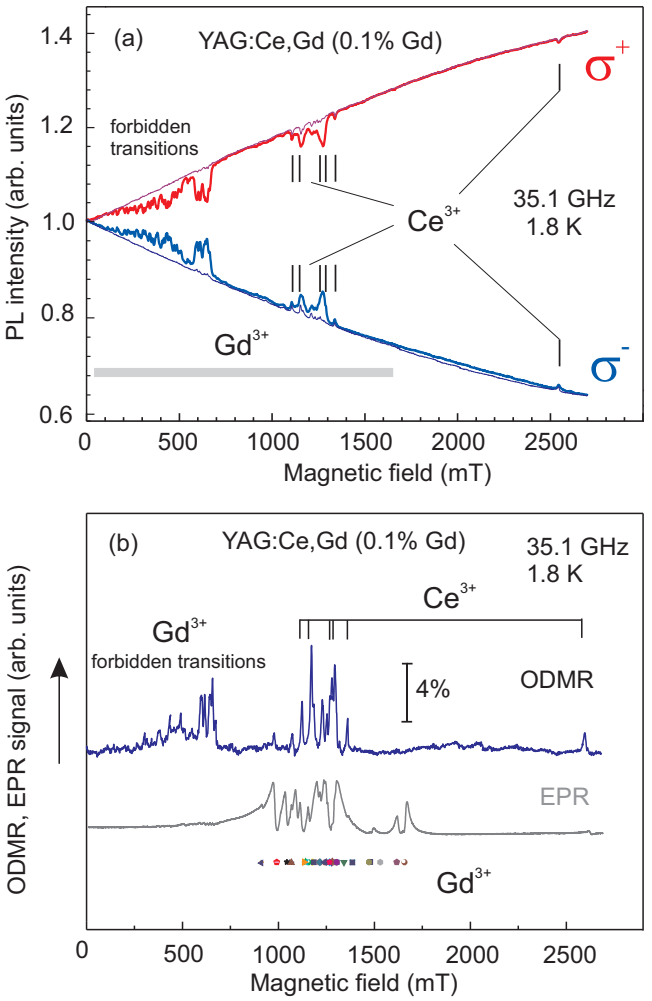

FIG. 4. (a) Magnetic field dependencies of the Ce^{3+} PL intensity in $Y_3Al_5O_{12}$:Ce,Gd (0.1% Gd) crystal measured at 1.8 K in the presence of the 35.1-GHz microwave field. 405-nm excitation light was circularly polarized (σ^+ or σ^-) as marked in the figure. Thick and thin lines correspond to different levels of the microwave power: 50 and 0.05 mW, respectively. The crystal orientation is close to $[110] \| B$. The magnetic field range where EPR of Gd^{3+} is expected is marked at the bottom. (b) Comparison of the baseline-corrected ODMR spectra recorded in $Y_3Al_5O_{12}$:Ce, Gd (0.1%) crystal via the Ce^{3+} PL intensity under σ^- excitation and the EPR spectrum recorded under the same conditions by monitoring the microwave power reflected from the cavity. Points at the bottom show the calculated positions of the allowed EPR transitions for Gd^{3+} at 35.1 GHz. The crystal orientation determined from the Ce^{3+} ODMR line positions corresponds to $\theta = 90°$, $\varphi = 35°$. $T = 1.8$ K. $\nu = 35.1$ GHz. ODMR signals of Ce^{3+} are marked. Additional ODMR lines belong to Gd^{3+}.

The baseline-corrected 35-GHz ODMR spectrum recorded by monitoring the PL intensity in YAG:Ce,Gd (0.1%) is shown in Fig. 4(b) together with the EPR spectrum measured on the same ODMR spectrometer by monitoring the microwave power reflected from the cavity. The sample orientation was determined from the Ce^{3+} ODMR spectrum and corresponded to $\theta = 90°$, $\varphi = 35°$. These spectra were recorded at a

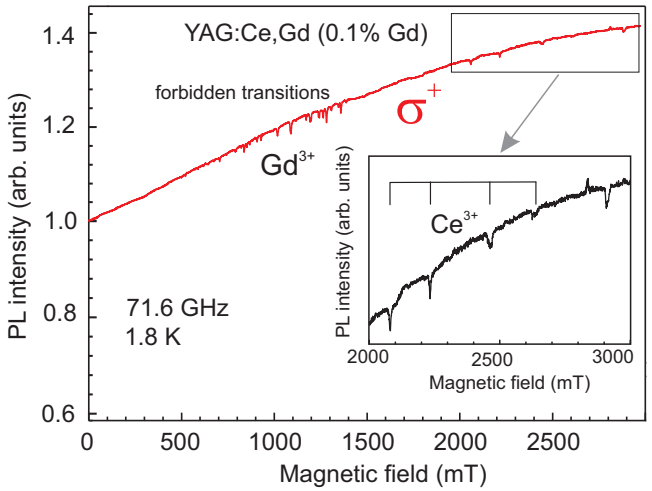

FIG. 5. Magnetic field dependencies of the Ce^{3+} PL intensity in $Y_3Al_5O_{12}$:Ce,Gd (0.1% Ce and 0.1% Gd) crystal measured at 1.8 K under 405-nm σ^+ excitation in the presence of the 71.6-GHz microwave field. Inset shows a part of the ODMR spectrum in enlarged scale. The crystal orientation is close to $\theta = 40^\circ$, $\varphi = 35^\circ$.

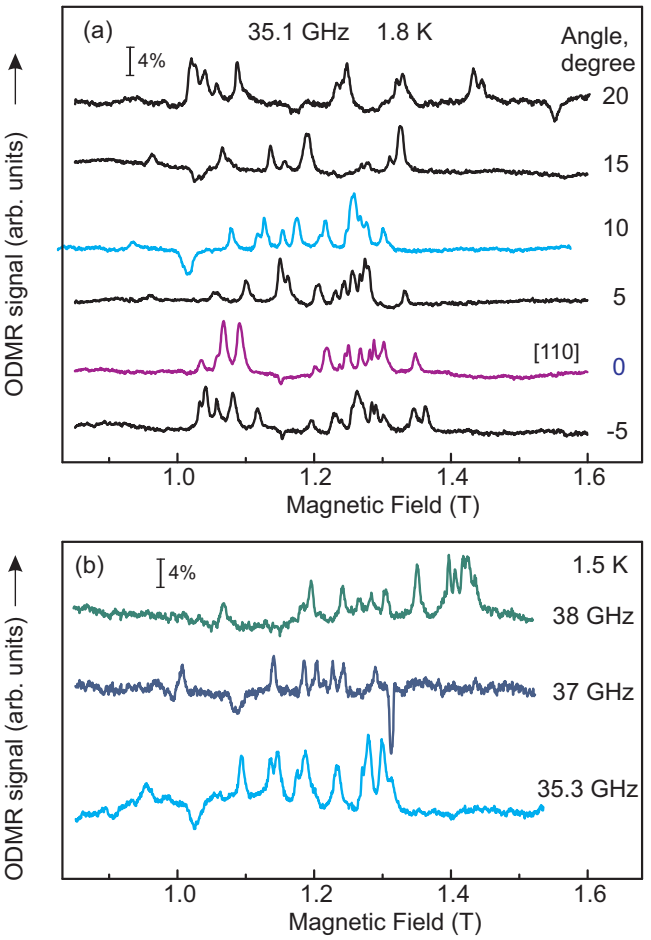

FIG. 6. A part of the baseline-corrected ODMR spectra recorded in $Y_3Al_5O_{12}$:Ce, Gd (0.1%) single crystal via the Ce^{3+} PL intensity under σ^- excitation at different orientations close to $[110] \| B$(a) and different microwave frequencies in the Q-band (b). 0 in (a) roughly corresponds to $[110] \| B$. The sample orientation in (b) is close to that marked as 10^o in (a).

microwave power of 5 mW with a slower field sweep and the sample orientation was slightly different from that of the spectra in Fig. 4(a). It is to be noted that in our ODMR spectrometer, the microwave frequency was fixed at 35.1 GHz and the sample was in the microwave cavity with an unloaded Q factor of about 3000. Therefore, the shape of the EPR signal is distorted by the dispersion signal.

One can see that in addition to the Ce^{3+} ODMR lines marked in Fig. 4(b) a number of ODMR signals that surely belong to the ground state of Gd^{3+} ions are observed. Gd^{3+} ions occupy the dodecahedral sites (c sites) and substitute for Y^{3+} ions in the crystal lattice. Calculations using (2) show that the 35-GHz EPR spectra of Gd^{3+} in YAG corresponding to the allowed $\Delta M = 1$ transitions should be observed in the magnetic field range of 0.88 to 1.68 T. In the ODMR spectra, however, only part of these EPR lines can be seen while a number of strong ODMR signals corresponding to the forbidden $\Delta M = 2,3$, etc., transitions are detected in the low field range.

The magnetic field dependence of the Ce^{3+} PL intensity in $Y_3Al_5O_{12}$:Ce,Gd (0.1% Gd) crystal measured at 1.8 K under 405-nm σ^+ excitation in the presence of the V-band (71.6 GHz) microwaves is shown in Fig. 5. Ce^{3+} ODMR lines and a number of forbidden transitions of Gd^{3+} shifted to higher field range are observed. Similar spectra, i.e., Ce^{3+} ODMR lines and forbidden transitions of Gd^{3+}, were observed in the W-band (94 GHz) ODMR. It should be noted that an increase in the microwave frequency may be useful to separate the Ce^{3+} and Gd^{3+} ODMR signals.

ODMR signals of Gd^{3+} recorded via Ce^{3+} luminescence are anisotropic and very sensitive to the crystal orientation and the microwave frequency. They can appear and disappear and even change sign with the rotation of the sample by a few degrees and variation of the microwave frequency as shown in Fig. 6.

In the sample under study, two different spin systems exist, i.e., Ce^{3+} and Gd^{3+}. Figure 7 shows a simplified scheme of the cross-relaxation coupling between these two systems, i.e., $S = \frac{7}{2}$ magnetic sublevels of Gd^{3+} and $S = \frac{1}{2}$ magnetic sublevels of Ce^{3+}. EPR transitions between a pair of the Gd^{3+} sublevels ($M_S = -\frac{7}{2}, -\frac{5}{2}, -\frac{3}{2}, -\frac{1}{2}, \frac{1}{2}, \frac{3}{2}, \frac{5}{2}, \frac{7}{2}$) can affect the electron spin polarization of Ce^{3+} if at the magnetic field corresponding to EPR of Gd^{3+} the energy separation between any pair of the Gd^{3+} levels with $\Delta M_S = 1$ ($\Delta M_S = 2,3\ldots$ for forbidden transitions) is close (within the EPR line width) to that between the Ce^{3+} levels $M_S = \pm\frac{1}{2}$ for one of six magnetically nonequivalent Ce^{3+} centers. If this is the case, the populations of the Gd^{3+} spin system can be transferred to the Zeeman levels of the Ce^{3+} centers due to cross relaxation, and change the cerium emission intensity.

In Fig. 7, two examples of possible cross-relaxation processes are shown for a certain orientation of the crystal in the magnetic field, i.e., cross relaxation between a pair of Ce^{3+} levels and a pair of Gd^{3+} levels that are involved in Gd^{3+} EPR (1) and cross relaxation between a pair of Ce^{3+} levels and a pair of Gd^{3+} levels that are not directly involved in Gd^{3+} EPR (2). Since saturation of EPR transitions between any pair

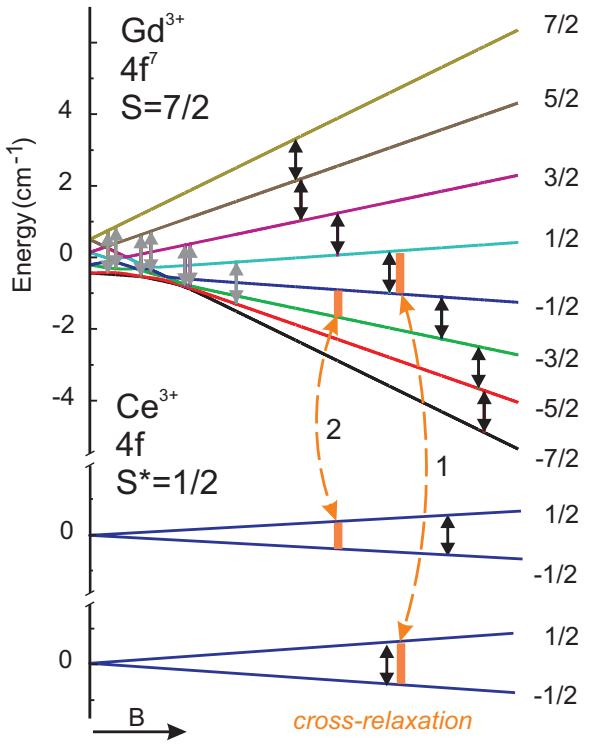

FIG. 7. A simplified scheme showing the energy levels and EPR transitions of Gd^{3+} and Ce^{3+} and two examples of Gd-Ce cross-relaxation transitions that change the Ce^{3+} spin polarization at EPR of Gd^{3+}.

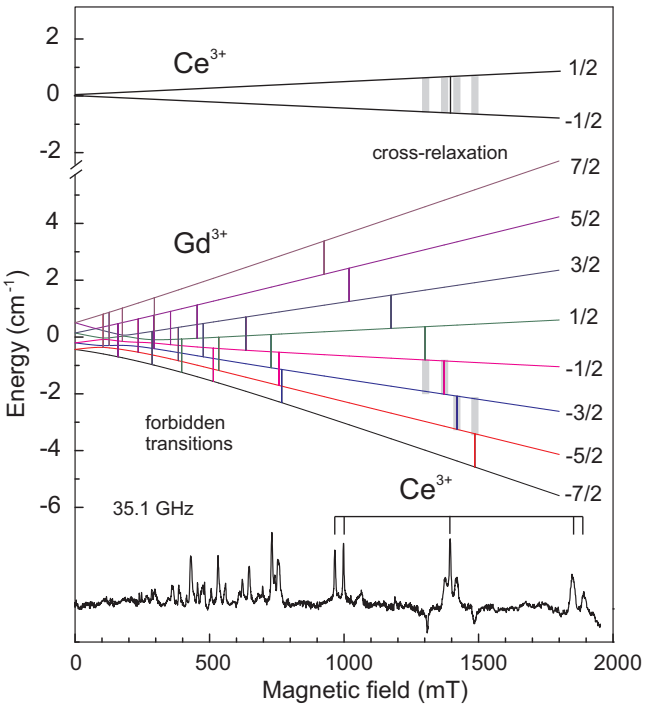

FIG. 8. Calculated energy levels and 35.1-GHz EPR transitions for one of six Gd^{3+} centers and one of six Ce^{3+} centers. $\nu = 35.1$ GHz, $T = 1.8$ K. Cross-relaxation transitions are marked by wide gray lines.

of Gd levels changes populations of all other levels it should change the Ce^{3+} spin polarization and affect the Ce^{3+} emission intensity.

The cross-relaxation conditions require that the energy splitting between a pair of the Gd^{3+} levels is close to that of a Ce^{3+} center and a finite overlap between their EPR lines exists. In a garnet crystal, there are six magnetically nonequivalent Gd^{3+} centers and six magnetically nonequivalent Ce^{3+} centers. In YAG:Ce,Gd (0.1 %) all EPR lines are narrow and cross relaxation appears in a narrow range of magnetic fields that can be outside the range of Gd^{3+} EPR. Therefore, only some of the possible Gd^{3+} EPR transitions can change the population of the Ce^{3+} ground-state levels and affect the Ce^{3+} PL intensity. The probability to observe Gd^{3+} ODMR due to cross relaxation is higher for forbidden Gd^{3+} EPR transitions since these take place in low magnetic fields (shaded arrows in Fig. 7) where the difference in the energy splitting of Gd^{3+} and Ce^{3+} levels is smaller.

An example of the ODMR spectrum in which the Gd^{3+} ODMR signals have different signs is given in Fig. 8 where the calculated energy levels for Ce^{3+} and Gd^{3+} centers are also displayed. Both allowed and forbidden 35-GHz EPR transitions are observed. The sample orientation determined from the positions of the Ce^{3+} ODMR lines ($\theta = 75°$, $\varphi = 18°$) was used for calculation of the energy levels for each of six Gd and Ce centers and for determining the cross-relaxation conditions. Only four Gd^{3+} lines are definitely seen in the range of allowed EPR transitions and they have different signs. They correspond to the calculated positions of EPR transitions for one of six Gd^{3+} centers described by Euler angles $\alpha = 45°$, $\beta = 90°$, $\gamma = 180°$. Calculations show that for these centers cross relaxation is possible with one of the Ce^{3+} centers described by Euler angles $\alpha = 135°$, $\beta = 90°$, $\gamma = 180°$. It was found that at magnetic fields corresponding to the four observed ODMR lines of Gd^{3+} cross relaxation may exist between the energy levels shown in Fig. 8 by thick gray lines.

Different signs of the ODMR signals can be explained by the schemes (A) and (B) in Fig. 9 where a central part of the ODMR spectrum of Fig. 8 recorded via the Ce^{3+} PL intensity under σ^- excitation, i.e., excitation from the $|+\frac{1}{2}\rangle$ level, is shown in enlarged scale. Positive signals correspond to an increase of the population, which can be caused by saturation of Ce^{3+} EPR or by cross relaxation with Gd^{3+}. The signs of the Ce^{3+} and Gd^{3+} ODMR signals are the same when the Gd EPR decreases the population difference between the Gd^{3+} levels $-\frac{3}{2} \leftrightarrow -\frac{1}{2}$ that are at cross resonance with the Ce^{3+} levels (A). The sign may be opposite if the Gd^{3+} EPR transition and cross-relaxation transitions occur between adjacent pairs of the Gd levels, i.e., $-\frac{1}{2} \leftrightarrow \frac{1}{2}$ and $-\frac{1}{2} \leftrightarrow -\frac{3}{2}$ (B).

For cross relaxation to appear it is necessary that there were an interaction between the two spin systems. Normally, this is a dipole-dipole interaction. Therefore, cross-relaxation effects are stronger in the samples with higher concentration of paramagnetic centers in which a sufficiently strong spin-spin interaction exists. It was shown [30] that measurements of cross relaxation can be used to estimate the intercenter separation. Cross relaxation between $S = \frac{7}{2}$ and $\frac{1}{2}$ spin systems has been studied in BaFBr:Eu phosphors (see [30,43] and references therein) where cross relaxation between Eu^{2+} and

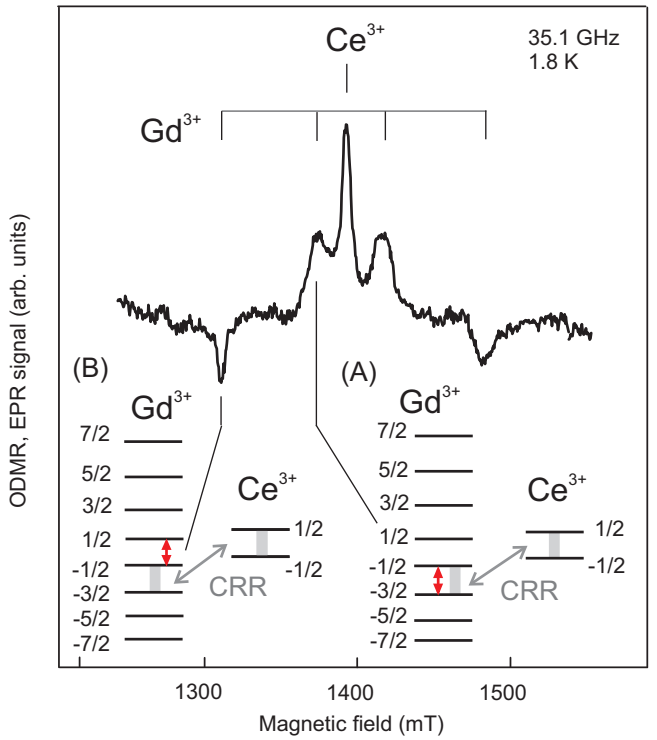

FIG. 9. Part of the ODMR spectrum of $Y_3Al_5O_{12}$:Ce, Gd (0.1%) shown in Fig. 8 and the energy-level schemes illustrating the Gd-Ce cross relaxation (CRR) resulting in different signs of the Gd^{3+} ODMR.

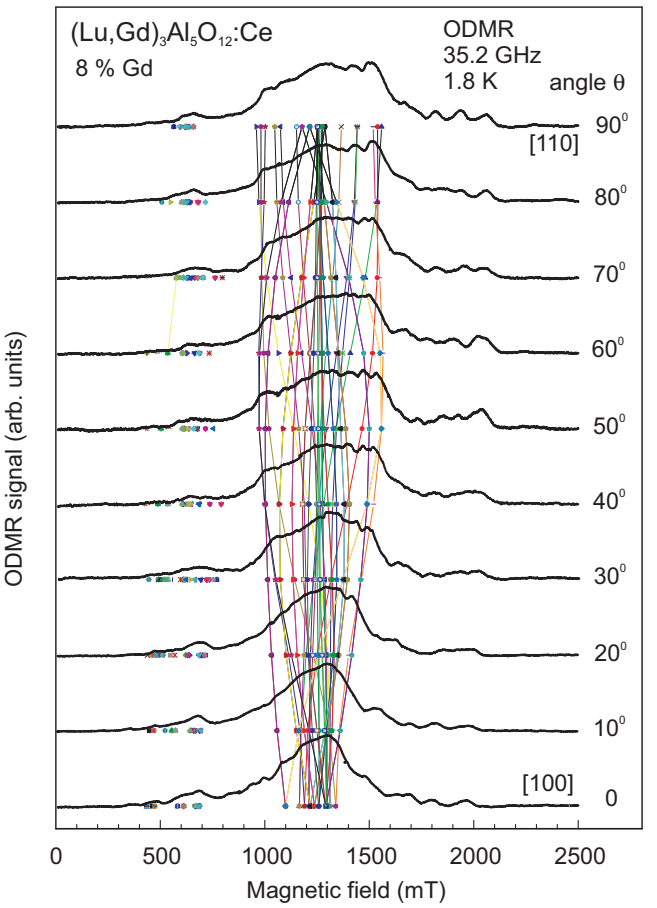

FIG. 10. Angular variations of the baseline-corrected 35.1-GHz ODMR spectra recorded via Ce^{3+} luminescence intensity in $Lu_{2.75}Gd_{0.25}Al_5O_{12}$:Ce crystals. The 405-nm excitation light was σ^- polarized, the rotation plane was close to (110). Points show the result of calculations of the Gd^{3+} EPR line positions. The ODMR lines in the high field range can be tentatively attributed to Gd-Gd pairs.

color centers was detected via MCD in optical absorption. In contrast to the Gd-Ce cross relaxation under study, the $S = \frac{1}{2}$ spin system in irradiated BaFBr:Eu crystals (F-centers) had an isotropic g factor. The anomalous behavior of the $S = \frac{7}{2}$ spin system in BaFBr:Eu was explained by the assumption that the spin-lattice relaxations within the Eu^{2+} energy levels operate faster for forbidden $\Delta M_S = \pm 2$ transitions than for allowed transitions [44].

3. *ODMR in (Lu,Gd)$_3$Al$_5$O$_{12}$:Ce crystals with medium concentration of Gd: (4% and 8%)*

ODMR of Gd^{3+} was also found by monitoring Ce^{3+} PL in $(Lu,Gd)_3Al_5O_{12}$:Ce crystals with medium concentration of Gd (4% and 8%). The Ce^{3+} concentration was about 0.1% as in all other samples under study.

Angular variations of the baseline-corrected ODMR spectra measured via Ce^{3+} luminescence in $(Lu,Gd)_3Al_5O_{12}$:Ce (8% of Gd) crystals in the same way as in YAG:Ce with low Gd content are shown in Fig. 10 together with the calculated angular dependencies of the Gd^{3+} EPR lines. Calculations were performed with Grachev's program [41] using spin Hamiltonian (2) with the EPR parameters for Ce^{3+} in LuAG listed in Sec. III B1. The ODMR lines are broadened due to high Gd concentration and the range of magnetic fields where cross-relaxation conditions can be fulfilled widens very much. The calculated dependencies for allowed EPR transitions are in good agreement with the central part of ODMR spectra.

In Fig. 11, ODMR spectra of $Lu_{2.875}Gd_{0.125}Al_5O_{12}$:Ce and $Lu_{2.75}Gd_{0.25}Al_5O_{12}$:Ce crystals, measured at the crystal orientation close to $B\|[110]$ are compared with the ODMR spectrum of $Y_3Al_5O_{12}$:Ce,Gd with low Gd content (0.1% Gd) shown at the bottom and gadolinium garnet $Gd_3Ga_3Al_2O_{12}$:Ce shown at the top.

One can see that aside from the main spectrum of Gd^{3+} additional ODMR lines in magnetic fields higher than 1.6 T are present. Calculations show that they cannot belong to single Gd^{3+} ions. The relative amplitudes of these lines increase in LuAG crystals with twice as high Gd content (8%) as compared to LuAG crystals containing 4% Gd. These signals have been tentatively ascribed to Gd-Gd pairs. They were not observed in the crystals with 0.1% Gd concentration. Recently, EPR of Ce^{3+} pair centers in $YAlO_3$:Ce scintillator crystals has been reported [45]. Aside from the single-ion Ce^{3+} spectrum, measurements have revealed many satellite lines which belong to the Ce^{3+}-Ce^{3+} pair centers. The spin-spin coupling constants were in the range from 0.1 up to 0.65 cm^{-1} depending on the distance between Ce ions and their position.

For such a high Gd content as 4% and 8% in our LuAG crystals, formation of Gd complexes including several Gd^{3+} ions coupled by spin-spin interaction starting from Gd^{3+}-Gd^{3+} pair centers is expected. For a Gd-Gd pair centers the EPR

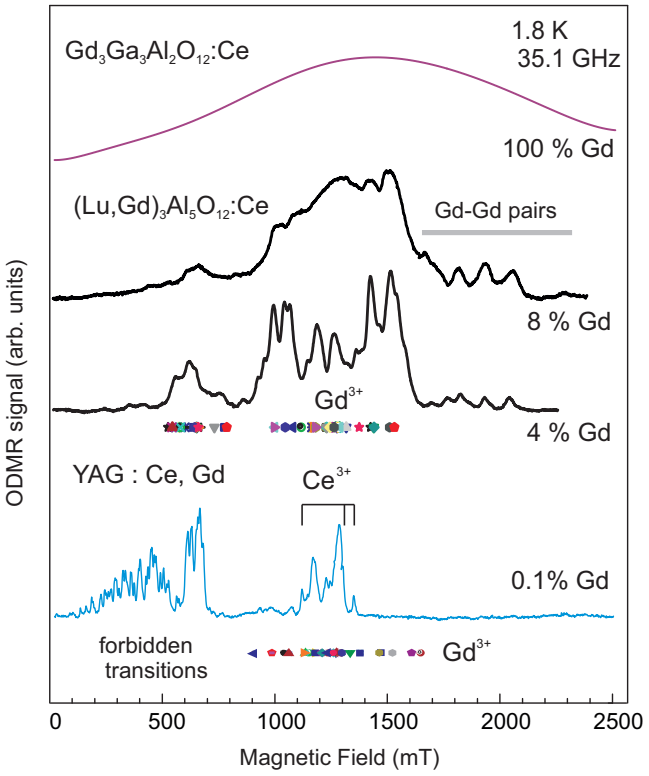

FIG. 11. The baseline-corrected 35.1-GHz ODMR spectra recorded via Ce^{3+} luminescence intensity in $(Lu,Gd)_3Al_5O_{12}$:Ce crystals with 4 at. % and 8 at. % of Gd relative to Lu. For comparison, the ODMR spectra of cerium-doped YAG:Gd (0.1% Gd) and gadolinium garnet ($Gd_3Ga_3Al_2O_{12}$) crystals are shown at the bottom and at the top of the figure, respectively. The 405-nm excitation light was σ^- polarized, the crystal orientation was close to $B \parallel [110]$.

transitions can be described by the spin Hamiltonian

$$\hat{H} = \hat{H}_{Gd1} + \hat{H}_{Gd2} + \vec{S}_1 \overleftrightarrow{J} \vec{S}_2, \quad (3)$$

where $\hat{H}_{Gd1}$ and $\hat{H}_{Gd2}$ are spin Hamiltonians (2) of both Gd^{3+} ions of a pair and $\overleftrightarrow{J}$ is the spin-spin interaction tensor including the contribution from both the dipole-dipole and exchange interactions.

Even for magnetically equivalent Gd ions, for which g and fine-structure tensors have the same principal axes as the spin-spin interaction tensor, calculations are difficult. For pairs that interact as magnetically nonequivalent ions, small off-diagonal terms in the spin Hamiltonian (3) are expected, which complicates calculations even more. From the positions of the additional lines in the ODMR spectra shown in Fig. 11 the spin-spin interaction value for Gd^{3+}-Gd^{3+} pairs can be roughly estimated as being of the order of 1 cm^{-1}, which is close to the spin-spin interaction parameters of Ce-Ce pairs in $YAlO_3$:Ce [45].

4. *ODMR and cross-relaxation effects in gadolinium garnet crystals $Gd_3Ga_3Al_2O_{12}$:Ce (100% Gd)*

The next step is an investigation of Ce-doped garnet crystals $Gd_3Ga_3Al_2O_{12}$ with 100% of gadolinium. A distinctive feature of Gd garnets is the presence of giant internal magnetic fields which occur near the Gd^{3+} ions and are caused by the magnetic moments of the unpaired electrons of the Gd^{3+} half-filled $4f$ shell [46,47]. An important physical task is to study how strong internal magnetic fields modify spin-dependent processes.

The curve at the top of Fig. 11 shows the baseline-corrected 35.1-GHz ODMR spectrum recorded in a Ce-doped gadolinium garnet crystal $Gd_3Ga_3Al_2O_{12}$ by monitoring the Ce^{3+} emission intensity under σ^--polarized 405-nm excitation, i.e., in the same way as the ODMR spectra in the garnet crystals with a small and medium Gd content shown in the same figure. A very wide unresolved ODMR line is observed. It should be emphasized that at any point within the magnetic field range where the ODMR spectrum is observed, the resonance absorption of the microwave power occurs due to EPR between spin sublevels of the gadolinium ions. It was shown [20] that at low temperature, the EPR line in a gadolinium garnet broadens due to increased magnetization and a wide distribution of local static fields.

Curves 1 and 2 in Fig. 12(a) show the magnetic field dependencies of the Ce^{3+} PL intensity measured with the 35-GHz microwave field switched on and off with a frequency of 0.1 Hz during the field sweep in $Gd_3Ga_3Al_2O_{12}$:Ce crystal for two different situations: (i) PL was excited by 405-nm σ^--polarized light (curve 1) and (ii) PL was excited by UV light of a deuterium arc lamp (curve 2). The sweep rate was 10 mT/s. The PL excitation conditions in the first case are similar to the ODMR measurements in the garnet crystals with low and medium Gd content described in the previous sections. Under σ^--polarized excitation the Ce^{3+} PL intensity increases when the resonant microwaves are applied and the PL variations follow the chopped microwaves. The transient behavior of the PL response to the applied microwaves is very different in the case of UV excitation. The inset in Fig. 12(a) shows a different shape of the PL response to the modulated microwave field for these two cases in enlarged scale. Very strong spikes corresponding to an increase in the PL intensity appear at the moments when the microwave field is switched off. The spike amplitude increases if the time interval when the microwaves are off becomes longer as shown at the bottom of the inset. The amplitude of the PL response to the applied microwaves is the ODMR signal of Gd^{3+} and its field dependence is similar to the ODMR spectrum shown in Fig. 11 (line at the top).

The observed difference for the cases of 405-nm and UV excitation can be explained by the fact that under 405-nm σ^--polarized excitation into the absorption band of Ce^{3+} ions the PL intensity monitors the population of the $|+\frac{1}{2}\rangle$ spin sublevel of Ce^{3+} and the microwave-induced variations of the PL intensity reflect variations of the Gd spin polarization due to the Gd-Ce cross relaxation similar to what was considered in the previous sections for the low and middle gadolinium concentration.

UV irradiation of the Ce-doped garnets is known to create radiation centers, whose spin-dependent recombination is the reason of the long-lasting afterglow. Under UV excitation, Ce^{3+} emission is excited both directly into UV absorption bands of Ce^{3+} (270 and 338 nm) and due to the energy transfer from recombination of radiation-induced electron and hole centers to cerium ions resulting in Ce^{3+} emission. To understand the PL behavior under the action of the

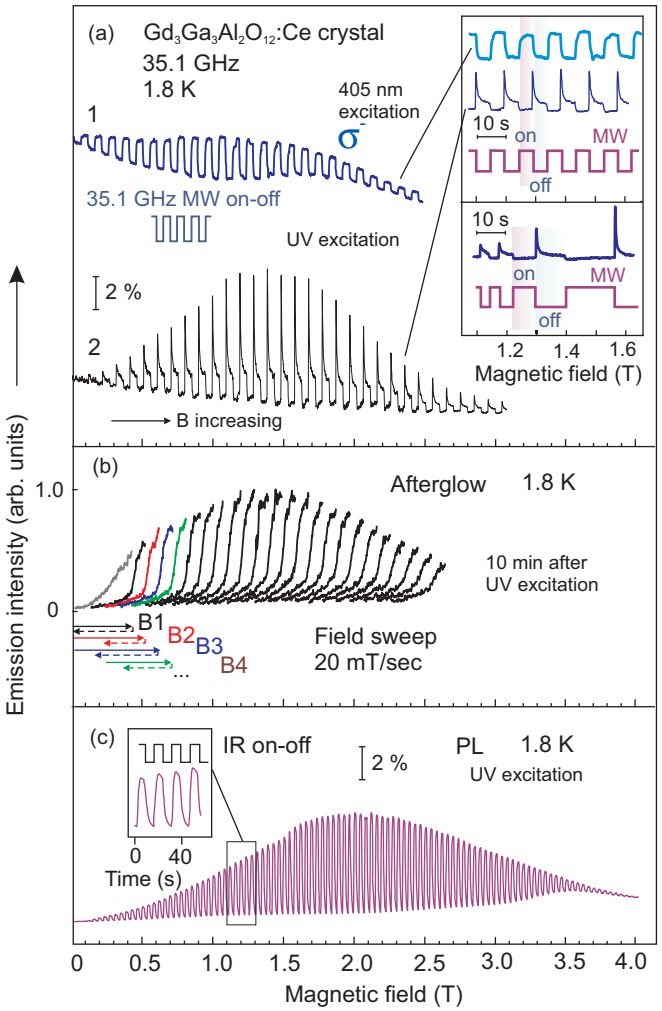

FIG. 12. (a) Magnetic field dependencies of the Ce^{3+} PL intensity in $Gd_3Ga_3Al_2O_{12}$:Ce crystal as a function of magnetic field measured with the 35-GHz microwave field switched on and off with a frequency of 0.1 Hz during the field sweep for two different situations: PL was excited by 405-nm σ^--polarized light (curve 1) and (ii) PL was excited by UV light of a deuterium arc lamp (curve 2). The sweep rate was 10 mT/s. Inset shows different shape of the PL response to the modulated microwave field for these two cases in enlarged scale. Strong spikes are observed at the moment of switching off the microwaves and their amplitude increases with time intervals when the microwaves are on. (b) A series of magnetic field dependencies of the afterglow emission intensity measured at 520 nm and 1.8 K in the same sample 10 min after UV irradiation. The magnetic field was swept from zero to a certain value and then reduced fast to a lower value as shown in the inset. In every second scan a sharp increase in the afterglow intensity appeared at the magnetic field value which corresponded to the maximum field in the previous scan. The sweep rate was 20 mT/s. (c) The field dependency of UV-excited PL in $Gd_3Ga_3Al_2O_{12}$:Ce recorded with additional near-IR (805-nm) photostimulation switched on and off with a frequency of 0.2 Hz during the field scan. The sweep rate was 10 mT/s. $T = 1.8$ K.

microwaves presented by curves 1 and 2 in Fig. 12(a), let us consider first the effects that have been previously observed via tunneling afterglow in UV-irradiated gadolinium garnets without application of the microwave field and without optical excitation in the process of measurement [34].

Figure 12(b) shows a series of the magnetic field dependencies of the afterglow intensity in $Gd_3Ga_3Al_2O_{12}$:Ce crystals measured at a temperature of 1.8 K ca. 10 min. after UV irradiation. In these measurements, the magnetic field was swept from zero to a certain value and then reduced fast to a lower value as shown in the inset in the bottom of the figure [34]. In every second scan, a sharp increase in the afterglow intensity appeared at the magnetic field value which corresponded to the maximum field in the previous scan.

Afterglow of preliminarily irradiated crystals is caused by recombination of trapped electrons and holes, i.e., electron and hole centers created by irradiation, and can last for a long time after irradiation. It is known that the efficiency of recombination of electron-hole pairs depends on the relative orientation of the spins of the recombination partners. Thus, the intensity of the recombination process is determined by the degree of spin polarization of the electron P_e and hole P_h centers in accordance with the known formula $I = I_0(1 - P_e P_h)$, where I_0 is the afterglow intensity in zero magnetic field, which is slowly reduced with time according to a hyperbolic law, P_e and P_h are electron spin polarizations of the electron and hole centers. Recombination is allowed when the spins of the electron and hole centers are oriented in the opposite directions, and is prohibited when they are lined up in the same direction. ODMR via tunneling recombination afterglow is based on this principle: at magnetic resonance of one of the recombining partners, the spin flip triggers an increase in the afterglow intensity [24].

We are interested only in the physical mechanism of the action of the magnetic field and the resonant microwave radiation on the recombination efficiency, i.e., on the reorientation of the spin of one of the recombining partners. Assume that initially the spins of the potentially recombining partners are mutually aligned so that their magnetic moments are oriented in the same direction along the local magnetic field at their positions. Recombination for them is forbidden. All other electron-hole pairs with opposite spins recombine during UV exposure or immediately after turning off the UV light, so only pairs with the same orientation of the spins remain. To allow their recombination, it is necessary to reorient the spin of one of the partners, that is, to induce either EPR transitions for an electron or hole center or to induce the cross relaxation of Gd^{3+} with one of the potentially recombining partners.

A simplified scheme illustrating Ce^{3+} excitation via the energy transfer from recombining e-h pairs and the effect of cross relaxation between Gd^{3+} and $S = \frac{1}{2}$ spin systems of electron and hole centers is shown in Fig. 13. For example, the two middle levels ($M_S = -\frac{1}{2}$ and $+\frac{1}{2}$) of Gd^{3+} are coupled to the electron center, therefore, only the spin occupancy of these two Gd^{3+} levels is important for the cross relaxation. The change in the occupancy of these two Gd^{3+} spin levels is transferred to the Zeeman levels of the electron or hole center by cross relaxation. It should be noted that the population of the $M_S = -\frac{1}{2}$ and $+\frac{1}{2}$ spin levels of Gd^{3+} is also influenced indirectly by relaxation within the Gd^{3+} $S = \frac{7}{2}$ spin system, that is, by EPR transitions between other Gd^{3+} levels. In a superparamagnetic material, the EPR spectrum in the form of a number of Gd^{3+} lines passes into a continuous broad EPR signal and there are resonant EPR transitions for Gd^{3+} ions at any magnetic field within this broad line.

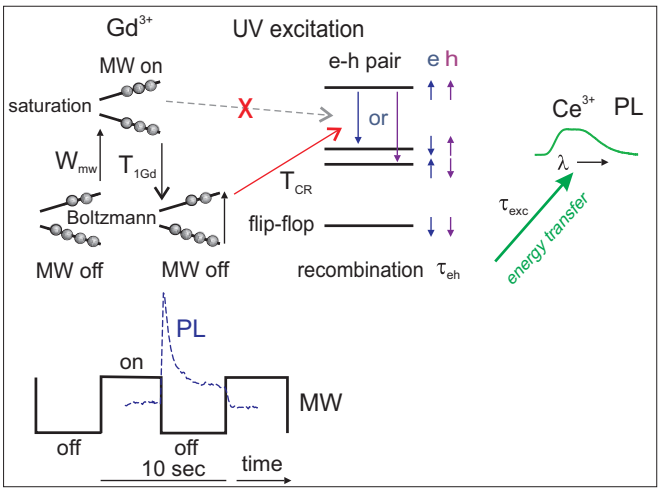

FIG. 13. A scheme explaining excitation of Ce^{3+} emission by the energy transfer from recombining e-h pairs in case of UV excitation and the effect of cross relaxation between the Gd^{3+} spin system and an $S = \frac{1}{2}$ system such as the electron (hole) color centers. Details are given in the text.

Saturation of Gd EPR transitions, i.e., equalization of populations of the Gd^{3+} spin sublevels, apparently suppresses the cross-relaxation-induced spin flips. As a result, accumulation of electron-hole pairs with parallel spins happens. The origin of the transient spikes in ODMR measurements with microwaves chopping can be readily explained since, in the presence of microwaves, a large population builds up in the electron-hole pairs, for which recombination is forbidden. As soon as the microwave field is switched off, the population of Gd^{3+} spin sublevels is redistributed via energy transfer to the lattice with the spin-lattice relaxation time T_{1Gd} and tends to the Boltzmann distribution. The cross relaxation will be switched on for the spin levels of one of the recombining partners for which the separation between the spin sublevels coincides with the corresponding separation between the Gd^{3+} spin sublevels. The spin orientation of one of the recombining partners will change and the excess recombination energy will be dumped into the emitting states of Ce^{3+}. A large and sudden increase in emission occurs, followed by a slow decrease to the new equilibrium value.

Summarizing, we can distinguish two physical processes underlying the spin-dependent phenomena in cerium-doped gadolinium garnet crystals, which affect the luminescence of Ce^{3+} ions. The first one is detection of the Gd^{3+} EPR via Ce^{3+} emission upon excitation of the EPR transitions between spin sublevels of Gd^{3+} ions, followed by cross relaxation with Ce^{3+} ions, which results in variation of populations of the Ce^{3+} spin sublevels. The nature of the processes occurring in this case is the same for garnet crystals with a low concentration of Gd^{3+} (0.1% of the Gd^{3+} ions replacing nonparamagnetic ions Y^{3+} or Lu^{3+} in YAG and LuAG, respectively), with a medium concentration of Gd^{3+} ions (4%–8%) and the highest possible concentration of Gd^{3+} ions (100%). In all cases, the excitation of Ce^{3+} PL was performed by circularly polarized light within the Ce^{3+}absorption bands in the range of 400–420 nm.

The result is that the ODMR spectrum repeats the EPR spectrum of the Gd^{3+} ions. For a low Gd concentration this is a set of narrow lines, and not all possible EPR transitions are observed in the ODMR spectrum. For a medium Gd concentration, the ODMR lines are broadened, and more EPR transitions of Gd^{3+} can be seen in the ODMR spectrum. The ODMR signals, which can be ascribed to the complexes of Gd^{3+} ions, appear. For the maximum Gd concentration, a broad structureless line is observed, which is explained by strong internal magnetic fields on the gadolinium ions, caused by adjacent magnetic ions. It is to be noted that under the action of UV light, direct excitation of luminescence in the Ce^{3+} absorption bands is also possible and, consequently, there exist all the effects of the cross-relaxation ODMR and above.

The second physical process is realized under UV excitation. The electron and hole centers formed as a result of UV irradiation can recombine and transfer the recombination energy to Ce^{3+} ions, which leads to the luminescence of these ions. The mechanisms of energy transfer from the recombining partners to Ce^{3+} ions are well known (see, for example, [3]), and are therefore not discussed in this paper. The presence of local magnetic fields caused by Gd^{3+} ions leads to significant changes in the processes of recombination of electron-hole pairs, and especially these effects are manifested in the structures with the maximum concentration of gadolinium ions, i.e., gadolinium garnets. These effects are manifested in a wide range of magnetic fields, which is close to the range of the EPR signals observed in gadolinium garnets. It should be emphasized that any electron-hole pair that is created by ionizing (UV) radiation in a gadolinium garnet is in the magnetic fields generated by gadolinium ions.

The energy stored after UV irradiation can also be released by infrared (IR) photostimulation. Such a photostimulation can change both the spatial distribution of the trapped electron and holes and their spin orientation and enhance their recombination. Figure 12(c) shows the PL response in Ce^{3+} PL in $Gd_3Ga_3Al_2O_{12}$:Ce on the additional IR 805-nm illumination that was switched on and off during the field sweep.

The microwave-induced variations of the Ce^{3+} PL intensity (ODMR) and the effect of IR photostimulation as far as the magnetic field enhancement of the afterglow intensity are observed in a very large field range, which can be explained by high magnetization at low temperature in the gadolinium garnet crystals and a distribution of internal magnetic fields. The fact that all these effects depend on magnetic field means that radiation-induced defects involved are paramagnetic.

Observation of spikes in cross-relaxation-induced ODMR signals under pulsed microwave excitation can be suggested as a method to investigate transient processes in the multispin system including Ce^{3+}, Gd^{3+} and electron and hole recombining partners. As was discussed above, in contrast to the case of simply optical excitation into the absorption bands of Ce^{3+} ions, when only two spin systems, i.e., Ce^{3+} and Gd^{3+} ions, interact, in the case of UV excitation, electron and hole centers that also possess spin moments are additionally formed. As a result, there are complex processes of energy transfer between different spin systems, characterized by different rate parameters, that is, with different transition probabilities between spin states.

The static and dynamic behavior of the spin systems and, thus, ODMR effects, can be described by a system of rate equations which consists of a differential equation system.

The transition rates between the spin levels are characterized by the spin-lattice relaxation time for each spin center, the EPR transition probability, the cross-relaxation time, the transition rate for the energy transfer from electron-hole recombination to an excited state of the Ce^{3+} emitters. Cross relaxation is especially efficient if the cross-relaxation time T_{CR} is of the order of an electron (hole) center spin-lattice relaxation time T_{1e} (T_{1h}) or smaller. The influence of the cross relaxation on the recombination of the UV radiation-induced electron and hole centers is increased by a short relaxation time T_{1Gd} within the Gd^{3+} spin system compared with the electron (hole) spin-lattice relaxation time T_{1e} (T_{1h}). It is more favorable for the transfer of the Gd^{3+} EPR effect by cross relaxation if the relaxation rate of the Gd^{3+} spin system is small in comparison with the EPR transition rate. As a result, EPR transitions within the Gd^{3+} system move this system far away from the thermal equilibrium and thus the spin occupancy of the levels is influenced greatly by the EPR transition.

An important result obtained at this stage is a fast (on the order of milliseconds) rise time of the spike signal followed by a slow relaxation. On the basis of this observation, it can be concluded that the processes leading to the appearance of the Gd^{3+} ODMR signal are fairly fast and the characteristic times, namely, the EPR transition time T_{MW} when the resonant microwaves are switched on, the Gd^{3+} spin-lattice relaxation time T_{1Gd}, the cross-relaxation time T_{CR}, the electron-hole recombination time τ_{eh}, and the time of the recombination energy transfer to the system of cerium ions τ_{exc} are in the range of 0.1 s or shorter. A relatively slow relaxation of the ODMR signal on the order of a few seconds after turning off the microwave power and the appearance of a spike seem to be due to spin-lattice relaxation in the system of electron and hole color centers for their transition to a new spin state under the action of optical excitation and spin-dependent recombination in new local magnetic fields. Pulsed EPR and ODMR studies are planned, which could help to obtain the whole set of characteristic times.

IV. CONCLUSIONS

An increase or decrease of the Ce^{3+} photoluminescence intensity in magnetic field has been found in cerium-doped single crystals at liquid-helium temperature depending on the sign of circular polarization of the excitation light. The circularly polarized excitation allows monitoring the population of one of the two Ce^{3+} ground-state spin sublevels via the PL intensity and to detect their variations due to both EPR of Ce^{3+} and cross relaxation of Ce^{3+} with Gd^{3+}.

Cross-relaxation effects have been studied in three types of gadolinium-containing garnets, i.e., YAG crystals with low Gd content (below 0.1 at. %), LuAG crystals with a medium Gd content (4 at. % and 8 at. %) and gadolinium garnets with 100% Gd. It was found that EPR in the ground state of Gd^{3+} ions changes the luminescence intensity of Ce^{3+}. The observation of the EPR spectra of Gd^{3+} ions by monitoring of the Ce^{3+} luminescence in $Y_3Al_5O_{12}$, $Y_3Al_5O_{12}$:Ce,Gd (0.1% Gd), $Lu_{2.75}Gd_{0.25}Al_5O_{12}$ and $Lu_{2.875}Gd_{0.125}Al_5O_{12}$ single crystals doped with cerium have demonstrated the impact of the spin state of gadolinium ions on the optical properties of cerium.

In the ODMR spectra of LuAG crystals with a medium Gd content ($Lu_{2.75}Gd_{0.25}Al_5O_{12}$ and $Lu_{2.875}Gd_{0.125}Al_5O_{12}$) additional lines have been found, which can be ascribed to Gd^{3+}-Gd^{3+} pairs. The spin-spin interaction can be roughly estimated as being of the order of 0.1 cm^{-1}.

Strong internal magnetic fields and the cross-relaxation effects in superparamagnetic $Gd_3Ga_3Al_2O_{12}$:Ce crystals result in different transient behavior of Ce^{3+} photoluminescence under chopped microwaves when excited by visible and UV light, which is due to different Ce^{3+} excitation mechanisms, i.e., direct excitation in the absorption bands of Ce^{3+} and cerium excitation due to recombination of radiation-induced paramagnetic electron and hole centers followed by energy transfer to Ce^{3+}.

Our experiments demonstrate the possibility of controlling the properties of fluorescent emitters based on Ce^{3+} ions by changing the magnetic spin state of the adjacent magnetic ion. It may be especially important to control the single-photon sources based on cerium and other rare-earth elements in garnets. As a result, single Ce^{3+} ions can be selected in the immediate vicinity of which there is a single magnetic ion (e.g., Gd^{3+}).

ACKNOWLEDGMENT

This work has been supported by the Russian Science Foundation, RFBR Grant No. 16-02-00877, and Philips Healthcare.

[1] P. Schlotter, R. Schmidt, and J. Schneider, J. Appl. Phys. A **64**, 417 (1997).

[2] V. Bachmann, C. Ronda, and A. Meijerink, Chem. Mater. **21**, 2077 (2009).

[3] M. Nikl, V. V. Laguta, and A. Vedda, Phys. Status Solidi B **245**, 1701 (2008).

[4] C. Dujardin, C. Mancini, D. Amans, G. Ledoux, D. Abler, E. Auffray, P. Lecoq, D. Perrodin, K. Ovanesyan, and A. Petrosyan, J. Appl. Phys. **108**, 013510 (2010).

[5] R. Autrata, P. Schauer, Jos. Kvapil, and J. Kvapil, J. Phys. E: Sci. Instrum. **11**, 707 (1978).

[6] M. Moszynski, T. Ludziewski, D. Wolski, W. Klamra, and L. O. Norlin, Nucl. Instrum. Methods Phys. Res., Sect. A **345**, 461 (1994).

[7] R. Kolesov, K. Xia, R. Reuter, M. Jamali, R. Stohr, T. Inal, P. Siyushev, and J. Wrachtrup, Phys. Rev. Lett. **111**, 120502 (2013).

[8] P. Siyushev, K. Xia, R. Reuter, M. Jamali, N. Zhao, N. Yang, C. Duan, N. Kukharchyk, A. D. Wieck, R. Kolesov, and J. Wrachtrup, Nat. Commun. **5**, 3895 (2014).

[9] K. Xia, R. Kolesov, Ya Wang, P. Siyushev, R. Reuter, T. Kornher, N. Kukharchyk, A. D. Wieck, B. Villa, S. Yang, and J. Wrachtrup, Phys. Rev. Lett. **115**, 093602 (2015).

[10] A. G. Badalyan, G. V. Mamin, Yu. A. Uspenskaya, E. V. Edinach, H. R. Asatryan, N. G. Romanov, S. B. Orlinskii, P. G. Baranov, V. M. Khanin, H. Wieczorek, and C. Ronda, Phys. Status Solidi B **254**, 1600631 (2017).

[11] S. A. Altshuler and B. M. Kozyrev, *Electron Paramagnetic Resonance in Compounds of Transition Elements*, 2nd ed. (Wiley, New York, 1974).
[12] A. Abragam and B. Bleaney, *Electron Paramagnetic Resonance of Transition Ions* (Oxford University Press, Oxford, 1970).
[13] H. R. Lewis, J. Appl. Phys. **37**, 739 (1966).
[14] G. R. Asatryan, D. D. Kramushchenko, Yu. A. Uspenskaya, P. G. Baranov, and A. G. Petrosyan, Phys. Solid State **56**, 1150 (2014).
[15] A. Vedda, M. Martini, D. Di Martini, V. V. Laguta, M. Nikl, E. Mihokova, J. Rosa, K. Nejezchleb, and K. Blazek, Radiat. Eff. Defects Solids **157**, 1003 (2002).
[16] L. Rimai and G. A. deMars, J. Appl. Phys. **33**, 1254 (1962).
[17] S. A. Marshall, T. Marshall, and R. A. Serway, Phys. Status Solidi A **48**, 165 (1978).
[18] V. A. Vazhenin, A. P. Potapov, G. R. Asatryan, Yu. A. Uspenskaya, A. G. Petrosyan, and A. V. Fokin, Phys. Solid State **58**, 1627 (2016).
[19] V. A. Vazhenin, A. P. Potapov, G. R. Asatryan, A. V. Fokin, M. Yu. Artemov, A. G. Petrosyan, in *XXII International Conference on Optics and Spectroscopy of Condensed Matter* (Krasnodar, Russia, 2016), Abstract, p. 81 (in Russian).
[20] J. Barak, M. X. Huang, and S. M. Bhagat, J. Appl. Phys. **71**, 849 (1992).
[21] *Electron Paramagnetic Resonance*, edited by S. Geschwind (Plenum, New York, 1972).
[22] B. C. Cavenett, Adv. Phys. **30**, 475 (1981).
[23] J.-M. Spaeth, J. R. Niklas, and R. H. Bartram, *Structural Analysis of the Point Defects in Solids* (Springer, Berlin, 1992).
[24] Baranov and N. G. Romanov, Appl. Magn. Reson. **2**, 361 (1991).
[25] P. G. Baranov and N. G. Romanov, Appl. Magn. Reson. **21**, 165 (2001).
[26] H.-J. Reyher, B. Faust, B. Sugg, R. Rupp, and L. Ackermann, J. Phys.: Condens. Matter **9**, 9065 (1997).
[27] H.-J. Reyher, N. Hausfeld, M. Pape, J. Baur, and J. Schneider, Solid State Commun. **110**, 345 (1999).
[28] N. Bloembergen, S. Shapiro, P. S. Pershan, and J. O. Artman, Phys. Rev. **114**, 445 (1959).
[29] E. S. Sabbisky, P. J. Call, and C. H. Anderson, Rev. Sci. Instr. **46**, 1632 (1975).
[30] J.-M. Spaeth and H. Overhof, *Point Defects in Semiconductors and Insulators* (Springer, Berlin, 2003).
[31] N. G. Romanov, V. V. Dyakonov, V. A . Vetrov, and P. G. Baranov, Fiz. Tver. Tela **31**, 106 (1989) [Sov. Phys.–Solid State **31**, 11 (1989)].
[32] M. Glasbeek and R. Hond, Phys. Rev. B **23**, 4220 (1981).
[33] K. M. Lee and G. D. Watkins, Phys. Rev. B **26**, 26 (1982).
[34] N. G. Romanov, D. O. Tolmachev, A. S. Gurin, Yu. A. Uspenskaya, H. R. Asatryan, A. G. Badalyan, P. G. Baranov, H. Wieczorek, and C. Ronda, Appl. Phys. Lett. **106**), 262404 (2015).
[35] A. S. Gurin, D. D. Kramushchenko, Yu. A. Uspenskaya1, G. R. Asatryan, A. G. Petrosyan, D. O. Tolmachev, N. G. Romanov, and P. G. Baranov, J. Phys.: Conf. Series **661**, 012039 (2015).
[36] N. G. Romanov, D. O. Tolmachev, A. S. Gurin, Yu. A. Uspenskaya, E. V. Edinach, H. R. Asatryan, A. G. Badalyan, P. G. Baranov, A. G. Petrosyan, H. Wieczorek, and C. Ronda, Appl. Magn. Reson. **47**, 73 (2016).
[37] A. A. Chernov, E. I. Givargizov, Kh. S. Bagdasarov, V. A. Kuznetsov, L. N. Demyanets, and A. N. Lobachev, *in Modern Crystallography*, edited by B. K. Vainshtein (Nauka, Moscow, 1980).
[38] A. G. Petrosyan, J. Cryst. Growth **139**, 372 (1994).
[39] R. A. Babunts, A. G. Badalyan, N. G. Romanov, A. S. Gurin, D. O. Tolmachev, and P. G. Baranov, Tech. Phys. Lett. **38**, 887 (2012).
[40] D. S. Hamilton, S. K. Gayen, G. J. Pogatshnik, R. D. Ghen, and W. J. Miniscalco, Phys. Rev. B **39**, 8807 (1989).
[41] V. G. Grachev, Zh. Eksp. Teor. Fiz. **92**, 1834 (1987) [Sov. Phys.–JETP **65**, 1029 (1987)].
[42] N. M. Atherton, *Principles of Electron Spin Resonance* (Prentice Hall, New York, 1993).
[43] F. K. Koschnik, J.-M. Spaeth, and R. S. Eachus, J. Phys.: Condens. Matter **4**, 8919 (1992).
[44] F. K. Koschnick, M. Rac, J.-M. Spaeth, and R. S. Eachus, J. Phys.: Condens. Matter **5**, 733 (1993).
[45] M. Buryi, V. V. Laguta, E. Mihokova, P. Novak, and M. Nikl, Phys. Rev. B **92**, 224105 (2015).
[46] *Hyperfine Interactions*, edited by A. J. Freeman and R. B. Frankel (Academic, New York, 1967).
[47] R. E. Watson and A. J. Freeman, Phys. Rev. **123**, 2027 (1961).